Analysis of Turbulent Transport Driven by Drift Alfvén Ballooning Mode

M. Uchida and A. Fukuyama

Department of Nuclear Engineering, Kyoto University, Kyoto, Japan

In order to realize high performance operation of fusion reactor, development of a reliable and robust transport model for burning plasmas is one of the key issues in fusion research. Transport models based on the ion temperature gradient (ITG) mode turbulence have recently attracted most attentions. We have proposed the current diffusive ballooning mode (CDBM) model [1], and successfully reproduced the L-mode confinement time scaling and the formation of internal transport barrier (ITB) [2,3].

Though these microscopic modes, such as ITG and CDBM, have been studied independently, it is desirable to give a unified view and clarifies the applicable range of these models. As a first step of this approach, we introduce a set of reduced two-fluid equations which describes both the electrostatic ITG mode and the electromagnetic ballooning mode including CDBM.

Starting from the full set of two-fluid equations for electrons and ions, we have derived the reduced two-fluid equation, which is composed of six equations, the equation of vorticity, parallel component of the equations of motion for electrons and ions, equations of state for electrons and ions, and Amperes law.

$$\left[\frac{n_{\rm i}\Lambda_0}{\Omega_{\rm i}B_0}-\frac{n_{\rm e}\Lambda_{0\rm e}}{\Omega_{\rm e}B_0}-\frac{\epsilon_0}{e}\right]\frac{\partial\nabla_\perp^2\phi_1}{\partial t}+\frac{n_{\rm i}}{\Omega_{\rm i}B}\frac{\partial}{\partial t}\left(\frac{\nabla_\perp^2 p_{1\rm i}}{q_{\rm i}n_{\rm i}}\right)-\frac{n_{\rm e}}{\Omega_{\rm e}B}\frac{\partial}{\partial t}\left(\frac{\nabla_\perp^2 p_{1\rm e}}{q_{\rm e}n_{\rm e}}\right)$$
$$-\nabla_\parallel(n_{\rm i}v_{1\parallel\rm i}-n_{\rm e}v_{1\parallel\rm e})+\left(\frac{{\rm i}en_{\rm i}\Lambda_{0\rm i}\omega_{*\rm i}}{T_{\rm i}}+\frac{{\rm i}en_{\rm e}\Lambda_{0\rm e}\omega_{*\rm e}}{T_{\rm e}}\right)\phi_1$$
$$=\frac{1}{eB}\left(\boldsymbol{b}\times\boldsymbol{\kappa}+\boldsymbol{b}\times\frac{\nabla B}{B}\right)\cdot(\nabla p_{1\rm i}+\nabla p_{1\rm e}) \tag{1}$$
$$m_j n_{0j}\frac{\partial v_{1j\parallel}}{\partial t}+\nabla_\parallel p_{1j}-q_j n_{0j}E_{1\parallel}=0 \tag{2}$$
$$\frac{\partial p_{j1}}{\partial t}+\boldsymbol{v}_{E1}\cdot\nabla p_{j0}+\Gamma_j p_{j0}\nabla_\parallel v_{\parallel j1}=0 \tag{3}$$
$$\nabla_\perp^2 A_{1\parallel}=-\mu_0\sum_j(n_0 q_j v_{1j\parallel}) \tag{4}$$

where Ω_j is the cyclotron frequency, Λ_0 represents the finite gyroradius effect, Γ_j is the specific heat, $\boldsymbol{\kappa}$ is the magnetic curvature, j = e or i denotes electron and ion, and other notations are standard. The equation of vorticity was obtained by combining the continuity equation, the perpendicular component of the equations of motion, and the Poisson equation with the assumption of $\omega \ll \Omega_{\rm i}$.

In a sheared slab geometry, the reduced two-fluid equations were solved numerically as an eigenvalue problem. The linear stability of the slab ITG mode was reproduced including the effect of electron temperature gradient.

In a toroidal configuration, we obtain the following set of equations after the transformation to the ballooning variable ξ.

$$\frac{-\mathrm{i}\omega}{\Omega_\mathrm{i}B_0}\frac{m^2}{r^2}f^2\left(n_{0\mathrm{i}}\Lambda_{0\mathrm{i}}\phi_1+\frac{p_{1\mathrm{i}}}{q_\mathrm{i}}\right)-\frac{-\mathrm{i}\omega}{\Omega_\mathrm{e}B_0}\frac{m^2}{r^2}f^2\left(n_{0\mathrm{e}}\Lambda_{0\mathrm{e}}\phi_1+\frac{p_{1\mathrm{e}}}{q_\mathrm{e}}\right)$$
$$-\frac{-\mathrm{i}\omega em^2f^2\phi_1}{\epsilon_0 r^2}+\frac{B_\theta}{rB_0}\frac{\partial}{\partial\xi}(n_{0\mathrm{i}}v_{1j\parallel}-n_{0\mathrm{e}}v_{1\mathrm{e}\parallel})-\frac{\mathrm{i}mB_\varphi}{erR_0B_0^2}H(\xi)(p_{1\mathrm{i}}+p_{1\mathrm{e}})=0 \quad (5)$$

$$-\mathrm{i}\omega m_j n_{0j}v_{1j\parallel}+\frac{B_\theta}{rB_0}\frac{\partial p_1}{\partial\xi}+q_j n_{0j}\left(\frac{B_\theta\Lambda_{0j}}{rB_0}\frac{\partial\phi}{\partial\xi}-\mathrm{i}\omega_{*aj}A_\parallel\right)=0 \quad (6)$$

$$-\mathrm{i}\omega p_{1j}-\mathrm{i}q_j n_{0j}\Lambda_{0j}\omega_{*j}(1+\eta_j)\phi+\frac{\Gamma_j p_{0j}B_\theta}{rB_0}\frac{\partial v_{1j\parallel}}{\partial\xi}=0 \quad (7)$$

$$-\frac{m^2}{r^2}f^2A_\parallel=-\mu_0 e(n_{0\mathrm{i}}v_{1\mathrm{i}\parallel}-n_{0\mathrm{e}}v_{1\mathrm{e}\parallel}) \quad (8)$$

where $H(\xi)\equiv\kappa_0+\cos\xi+(s\xi-\alpha\sin\xi)\sin\xi$ and $f^2(\xi)=1+(s\xi-\alpha\sin\xi)^2$, m is the poloidal mode number.

Figure 1 shows typical eigenfrequency and growth rate as a function of pressure gradient. When the pressure gradient is small, the growth rate is close to that of the toroidal ITG mode. With the increase of the pressure gradient, the electromagnetic effect becomes dominant and the mode deviates from the toroidal ITG mode. This

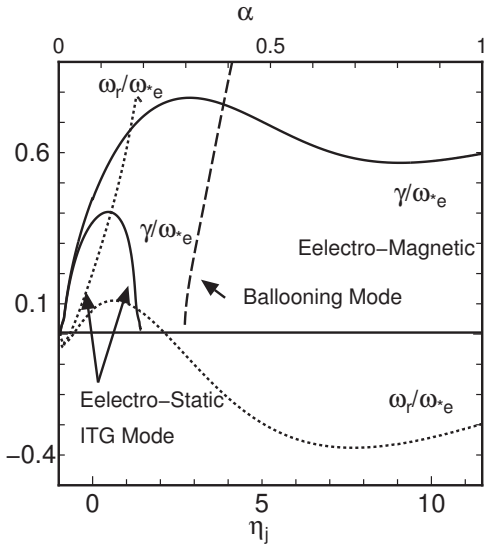

Figure 1 Eigenfrequency and growth rate of DABM as a function of pressure gradient for $\epsilon_n = L_n/R = 0.6/3 = 0.2$, $q = 2$, $k_\perp\rho_\mathrm{i} = 0.36$, $s = 0.4$, and $T_\mathrm{e}/T_\mathrm{i} = 1$

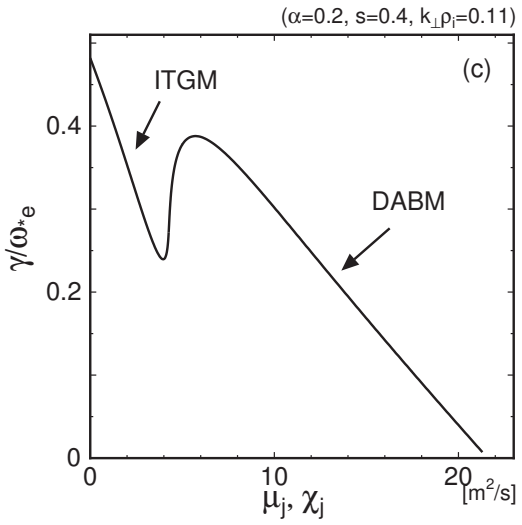

Figure 2 Growth rate of DABM as a function of the magnitude of transport coefficients. Parameters are $\rho_\mathrm{i} = 3.23\times10^{-3}\,\mathrm{m}$, $T_{\mathrm{i}0} = 1\,\mathrm{keV}$, $L_n = 0.6\,\mathrm{m}$, $R = 3\,\mathrm{m}$, $r = 0.532\,\mathrm{m}$, $m = 60$, $s = 0.4$, $q = 2$, and $c^2/(\omega_\mathrm{pe}^2r^2) = 10^{-5}$.

mode propagates in the direction of the ion diamagnetic drift and stays unstable where the ideal ballooning mode is unstable. Since this universal ballooning mode is related to both the ITG branch of the drift wave and the Alfvénic ballooning mode, we call it drift Alfvén ballooning mode (DABM).

In order to evaluate the turbulent transport coefficients, we employ the theory of self-sustained turbulence [4]. We introduce the electron viscosity $\mu_{\rm e}$ associated with the current diffusivity λ, the ion viscosity $\mu_{\rm i}$ and the thermal diffusivities, $\chi_{\rm e}$ and $\chi_{\rm i}$, into the reduced two-fluid model:

$$\left[(-{\rm i}\omega+\mu_{\rm i}\frac{m^2f^2}{r^2})\frac{n_{0{\rm i}}}{\Omega_{\rm i}B_0}-\frac{-{\rm i}\omega e}{\epsilon_0}-(-{\rm i}\omega+\mu_{\rm e}\frac{m^2f^2}{r^2})\frac{n_{0{\rm e}}}{\Omega_{\rm e}B_0}\right]\frac{m^2f^2}{r^2}\phi_1$$
$$+\left(-{\rm i}\omega+\chi_{\rm i}\frac{m^2f^2}{r^2}\right)\frac{1}{\Omega_{\rm i}B_0}\frac{m^2}{r^2}f^2\frac{p_{1{\rm i}}}{q_{\rm i}}-\left(-{\rm i}\omega+\chi_{\rm e}\frac{m^2f^2}{r^2}\right)\frac{1}{\Omega_{\rm e}B_0}\frac{m^2}{r^2}f^2\frac{p_{1{\rm e}}}{q_{\rm e}}$$
$$+\frac{B_\theta}{rB_0}\frac{\partial}{\partial\xi}(n_{0{\rm i}}v_{1j\|}-n_{0{\rm e}}v_{1{\rm e}\|})-\frac{{\rm i}mB_\varphi}{erR_0B_0^2}H(\xi)(p_{1{\rm i}}+p_{1{\rm e}})=0 \tag{9}$$
$$m_jn_{0j}\left(-{\rm i}\omega+\mu_j\frac{m^2f^2}{r^2}\right)v_{1j\|}+\frac{B_\theta}{rB_0}\frac{\partial p_1}{\partial\xi}+q_jn_{0j}\left(\frac{B_\theta\Lambda_{0j}}{rB_0}\frac{\partial\phi}{\partial\xi}-{\rm i}\omega_{*aj}A_\|\right)=0 \tag{10}$$
$$\left(-{\rm i}\omega+\chi_j\frac{m^2f^2}{r^2}\right)p_{1j}-{\rm i}q_jn_{0j}\Lambda_{0j}\omega_{*j}(1+\eta_j)\phi+\frac{\Gamma_jp_{0j}B_\theta}{rB_0}\frac{\partial v_{1j\|}}{\partial\xi}=0 \tag{11}$$
$$-\frac{m^2}{r^2}f^2A_\|=-\mu_0e(n_{0{\rm i}}v_{1{\rm i}\|}-n_{0{\rm e}}v_{1{\rm e}\|}) \tag{12}$$

The thermal diffusivities of electrons and ions stabilize the mode, while the ion parallel viscosity can destabilize the mode in the case of large pressure gradient. These transport coefficients are functions of the fluctuation amplitude. We assume that these coefficients are proportional to one parameter, e.g. χ. Figure 2 indicates the χ dependence of the growth rate. When χ is small, it has stabilizing effect on an ITG like mode. Above a critical value of χ, it destabilize an electromagnetic mode, mainly through the ion parallel viscosity.

From the condition that all modes with different poloidal mode numbers are stabilized, we have evaluated the transport coefficients driven by the DABM. Figure indicates the dependence on the magnetic shear s. Weak or negative magnetic shear reduces the transport coefficients. This behavior is similar to that of the CDBM which corresponds to neglect the compressibility and a part of the drift motion, but we should note that the magnitude of χ is more than one order of magnitude larger than that of CDBM. Since we need a multiplier of 12 in order to reproduce the experimental observation by the CDBM model [2,3], DABM is more appropriate for this typical set of parameters.

The dependence on the pressure gradient is shown in Fig. for various values of s. When the pressure gradient is small, χ is approximately proportional to $\alpha^{3/2}$. As α increases, *chi* starts to saturates. When the pressure gradient exceeds a critical value, however, χ starts to increase strongly with α, which may suggest the stiffness of the profile. In the case of negative s, transition from an electrostatic branch to an electro-

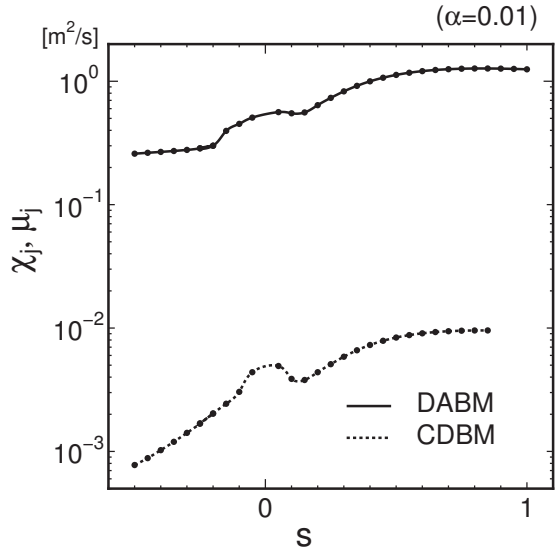

Figure 3 Magnetic shear dependence of the transport coefficients for DABM and CDBM. Parameters are similar to Fig. 2.

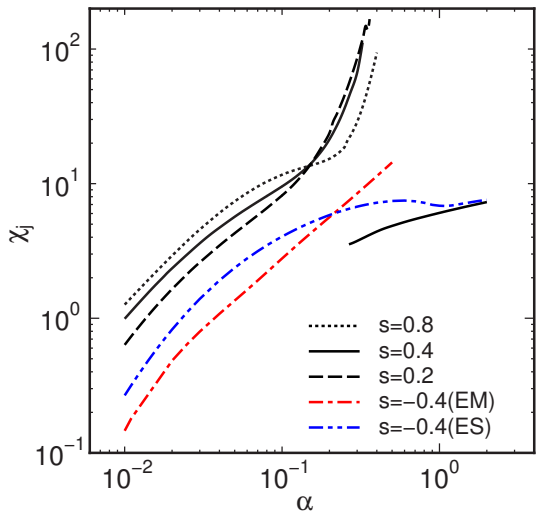

Figure 4 Pressure gradient dependence of the transport coefficients of DABM for various values of s. Parameters are similar to Fig. 2.

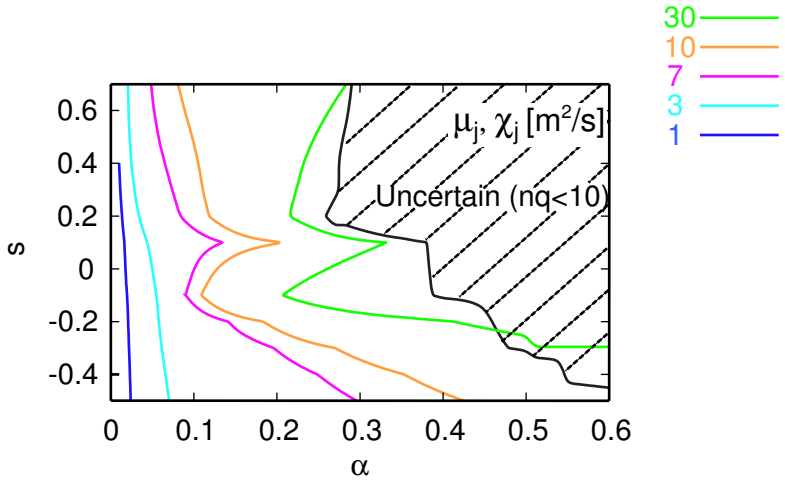

Figure 5 Contour plot of χ on the s-α plane. Parameters are similar to Fig. 2.

magnetic one, but the increase of χ is mild even in the large α region.

Finally, the s and α dependence of χ is shown in Fig. 5. We see reduction of χ in the low and negative s region. The present analysis is not applicable in the large α region where low-m modes become dominant and the marginal stability condition cannot be satisfied. This constraint should be removed in future. In conclusion, the DABM model is a promising candidate to explain the turbulent transport in tokamaks.

[1] K. Itoh et al.: Plasma Phys. Control. Fusion, **35** (1993) 543.
[2] A. Fukuyama et al.: Plasma Phys. Control. Fusion, **37** (1995) 611.
[3] A. Fukuyama et al.: Nucl. Fusion, **35** (1995) 1669.
[4] K. Itoh et al.: Plasma Phys. Control. Fusion, **36** (1994) 279.